arXiv:1211.1753v1 [cond-mat.mes-hall] 8 Nov 2012

Polariton condensation and photon lasing: photoluminescence features at low temperature and in high excitation regime

Tomoyuki Horikiri[1,2,3], **Yasuhiro Matsuo**[1,3], **Yutaka Shikano**[4], **Andreas Löffler**[5], **Sven Höfling**[1,5], **Alfred Forchel**[5], **Yoshihisa Yamamoto**[1,2]

[1]National Institute of Informatics, Hitotsubashi 2-1-2, Chiyoda-ku, Tokyo 101-8430, Japan,
[2]E. L. Ginzton Laboratory, Stanford university, Stanford, California 94305, USA
[3]The University of Tokyo, 7-3-1 Hongo, Bunkyo-ku, Tokyo 113-8656, Japan
[4]Institute for Molecular Science, 38 Nishigo-Naka, Myodaiji, Okazaki 444-8585, Japan
[5]Technische Physik, Universität Würzburg, Am Hubland, D-97074 Würzburg, Germany

E-mail: `tomoyuki-horikiri@nii.ac.jp`

Abstract. A polariton condensation has been observed in a microcavity semiconductor. In the low excitation regime, this can approximately be taken as the thermal-equilibrium. The higher the excitation is, the more dominant the non-equilibrium features are. In the high excitation regime, standard photon lasing is expected to take place because of its microcavity structure. In this paper, we report the crossover regime from polariton condensation to photon lasing by the temperature and excitation-density dependences. In the low temperature and the high excitation regime, we find a different behaviour of photoluminescence to photon lasing to be expected from the past studies.

PACS numbers: 71.36.+c, 67.85.Hj, 78.55.Cr, 78.67.De

1. Introduction

A polariton is a bosonic quasiparticle resulting from the strong coupling between a photon and an exciton. When an inflow rate to the ground state of the polariton exceeds the loss rate from the cavity, the final state stimulation can result in a macroscopic population of the ground state and the polariton can be condensed to the ground state [1, 2, 23]. This can be called the condensation threshold. This is experimentally confirmed by a nonlinear increase of photoluminescence (PL) from a semiconductor microcavity against an input pump power since the polariton inside the cavity cannot be directly observed. Due to the short lifetime of the polariton, this condensation is basically taken as non-equilibrium dynamical condensation [3]. However, it can be taken as the thermal-equilibrium condensation; the polariton Bose-Einstein condensation (BEC) [4] under some conditions.

There are many experimental evidences that the polariton condensation is the weakly interacting BEC induced by the polariton-polariton interaction. For examples, observation of a superfluidity [5], a vortex formation [6], a vortex-antivortex pair creation [7] and the spectrum of the Bogoliubov excitation [8]. Furthermore, the polariton condensation has a potential as a novel type of the laser with low input-power requirements [9]. Unlike the standard photon lasing in a semiconductor, this does not need population inversion. As the pump power increases, the polariton-polariton interaction also increases at first. At very high density, the overlap of excitons causes screening effect of coulomb interaction. Therefore, the binding of the electron-hole (e-h) pair breaks and the system becomes e-h plasma. The population inversion occurs and the photon lasing is observed after the second nonlinear increase, which is often called the second threshold in contrast to the above mentioned condensation threshold which can be also called the first threshold [10, 11, 12, 13, 14, 15, 16]. However, according to recent theoretical studies [17, 18, 19, 20], there still can be the e-h pair binding in the high density regime.

The aim of this paper is to demonstrate the different PL behaviour from the standard photon lasing in the high excitation regime. To pursue this aim, the temperature dependence of PL is investigated since the high-temperature case shows the standard photon lasing. Our main result is the demonstration of the completely different PL behaviour from standard photon lasing at the low temperature (8 K) in the high excitation regime.

This paper is organized as follows. In Sec. 2, we recapitulate basic concepts of the semiconductor microcavity polariton. Recent developments in the high density regime are reviewed in Sec. 3. In Sec. 4, the results of the excitation dependence measurements are shown where PL intensity, energy, PL linewidth and the second order correlation function are studied against the pump power. In the low temperature, we report a different regime, which cannot be understood as the standard photon lasing. Section 5 is devoted to summary and discussion in the high density regime.

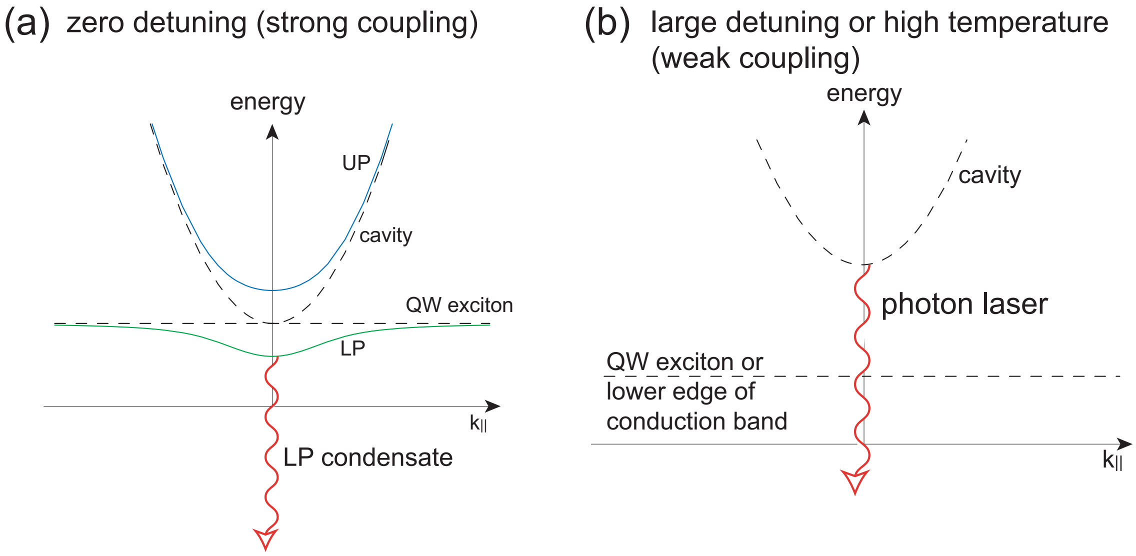
(a) zero detuning (strong coupling)
energy
UP
cavity
QW exciton
LP
$k_{||}$
LP condensate
(b) large detuning or high temperature (weak coupling)
energy
cavity
photon laser
QW exciton or lower edge of conduction band
$k_{||}$

Figure 1. Energy-momentum relations for strong coupling and weak coupling regimes. (a): polariton condensation. (b): photon lasing where population inversion is necessary.

2. Polariton Condensation and Photon Lasing

In this section, we recapitulate basic concepts of the polariton condensation compared to the standard photon lasing. As shown in Fig. 1a, a polariton in a semiconductor microcavity having quantum-well (QW) inside is created by the strong coupling between a QW exciton and a cavity photon where exciton is formed by binding between an electron and a hole. As the result of fast energy transfer between the two modes, the normal mode splitting occurs. Then, two energy branches called upper polariton (UP) and lower polariton (LP) are formed. Polariton condensate is formed on the LP ground state when the condensation threshold condition of the following requirement is fulfilled. The injection rate into the LP ground state through relaxation by e-h pairs', e-h and phonon, polariton-polariton and polariton-phonon scatterings is larger than the loss rate from the ground state due to the inverse processes and mainly cavity leakage. When the requirement is fulfilled, macroscopic population on the LP ground state is grown and PL non-linear increase is observed. From the requirement, the polariton condensate is often called the polariton laser. The difference from photon lasing is on the point that the strong PL emission is not caused by the usual mechanism of lasing, i.e., light amplification by stimulated emission of radiation.

On the other hand, a conventional semiconductor photon lasing, which is called the photon laser, as shown in Fig. 1b occurs at the cavity photon mode inside the conduction band, where there is no longer strong coupling between the cavity photon and the QW exciton. In room temperature, exciton dissociates due to the large thermal energy. Since the exciton level no longer exists in usual medium as GaAs, the cavity energy inside the conduction band needs to be fulfilled with e-h plasma. The photon lasing needs the

Table 1. Different features of polariton condensation and photon lasing. $\omega_{\rm cav}$ is the cavity photon energy, $\omega_{\rm LP}$ is the LP ground state energy, and μ is condensate blue-shift due to interactions.

	$g^{(2)}(0)$	energy level	linewidth
polariton condensate	> 1	$\omega_{\rm LP} + \mu$	becoming broad due to p-p interaction
photon laser	$\to 1$	$\omega_{\rm cav}$	narrowing due to cavity linewidth

population inversion against the crystal ground state. There are differences between polariton condensation and photon lasing. The normalized second-order correlation function $g^{(2)}(0)$ of photon lasing converges into unity just above the lasing threshold [21], while that of polariton condensate shows bunching ($g^{(2)}(0) > 1$) at wide area above the condensation threshold [3, 22]. This can be understood as results of interactions between condensate polaritons or between polariton and phonon. The polaritons are kicked out of the condensate as a result of interaction. The condensate population is depleted and shows super-Poissonian statistics [23, 24, 25, 26, 27]. Due to the mechanism, the higher-order coherence of the condensate is not realized. Actually, the third-order correlation function $g^{(3)}(0)$ has been observed and showed larger values $g^{(3)}(0) > g^{(2)}(0) > 1$ [28]. The coherent state must show all-order coherence $g^{(n)}(0) = 1$ while the thermal state shows $g^{(3)}(0) = 6 > g^{(2)}(0) = 2 > 1$. Consequently, PL from polariton condensate is not in the coherent state but close to the thermal state.

The differences between polariton condensation and photon lasing are summarised in Table 1. Other clear differences are the energy and linewidth, which are observable in PL measurements. In polariton condensation, PL energy remains basically on the LP ground state ($\omega_{\rm LP}$) though it shows small energy blue-shift due to polariton interactions (μ) while photon laser basically stays at the cavity photon energy of zero inplane-momentum ($\omega_{\rm cav}$). Polariton linewidth broadens as density increases also due to polariton-polariton (p-p) interactions [30], while photon laser shows very narrow linewidth since it does not have the polariton-polariton interaction mechanism.

3. Behaviours in high excitation regime

When a polariton system can reach the condensation regime above the condensation threshold, the system has shown the transition into a photon lasing at a high excitation regime where population inversion occurs in previous studies [10, 11, 12, 13, 14, 15, 16]. PL intensity has the second threshold of the nonlinear increase, and $g^{(2)}(0)$ is also monotonically converged to the unity [16]. These studies can be understood as follows. As increasing the e-h interaction in high excitation regime, the binding between e-h pair breaks and the exciton becomes e-h plasma. Consequently, standard photon lasing takes place after the gain for the cavity photon mode exceeds its loss. However, it is unclear whether the breaking of the e-h pair binding which is basically determined by the e-h interaction and the e-h density necessarily occurs in any sample or not. The polariton condensate is expected to experience several phases governed by excitation density and detuning, where the different signature to the photon laser has been theoretically pointed out under suitable conditions [17, 18, 19, 20]. Especially, Ref. [20] utilises the framework of a nonequilibrium system caused by pumping and decay [29] which is very close to the realistic experimental conditions. The above experimental studies have observed the transition to photon lasing in high density regime. In those works, polariton no longer survives. Exciton dissociates and becomes e-h plasma in the high excitation regime. However, the above theoretical works predicted that there should be another regime which does not necessarily experience e-h pair breaking in the high density regime. So there is discrepancy between theory and experiment at present. The experimental condition for implementing e-h pair binding at high density is not fixed yet. However, different parameter usage, for examples, different Q values of sample, detuning, excitation properties (angle, spot size and energy), and decreasing heating effect due to pumping laser, may contribute to observe the difference from photon lasing. In what follows, we report the PL behaviour by changing the temperature and the excitation density in the same sample. At least, our main results in the low temperature are not completely explained by the picture of transition to photon lasing and imply the effect due to e-h pair binding still remains.

4. Temperature and excitation density dependence of PL

In this section, we see the temperature and excitation density dependences of PL. As mentioned in the previous section, the low temperature condition where polariton condensate can be formed has the possibility showing a different behaviour from a photon laser. To compare the result with a photon lasing case, we also show high temperature measurements where e-h pairs dissociate due to thermal energy and cavity photon mode is inside the conduction band. Also additional experiments at intermediate temperatures show interesting behaviours including the second threshold of the transition from polariton condensate to photon laser, which inversely clarifies the absence of the second threshold at the low temperature.

4.1. Experimental setup

The sample has the microcavity structure consisting of AlAs/AlGaAs distributed Bragg reflectors (DBR). The number of top (bottom) layer is 16 (20) to obtain the PL from the top surface. Total 12 QWs are divided into 3 groups and positioned at the 3 highest mode intensity antinodes of the microcavity. This sample shows a strong coupling at low temperature and the normal mode splitting at $k = 0$ is 14 meV around zero detuning. A mode-locked Ti:Sapphire laser with 3 ps pulse width is utilized as a pump laser, and the laser is injected into the sample from $50 - 60^\circ$ from the normal which corresponds to $k_{||} \sim 7 \times 10^4$/cm. The pump laser wavelength is set to 747 nm at 8 K to maximize the

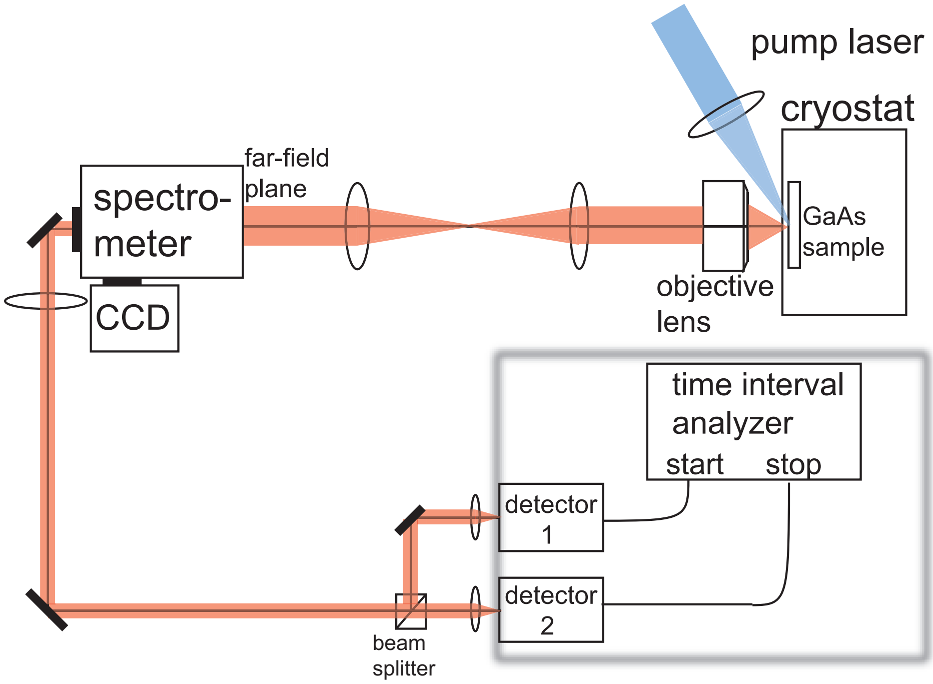

Figure 2. Experimental setup for dispersion relation measurements. Blue beam represents pump laser, while red represents PL from the sample.

injection rate into the sample reflection dip due to cavity photon mode. As temperature increases, the cavity photon energy experiences red-shift. Therefore, the pump laser wavelength needs to be changed with temperature.

The schematics of the experimental setup is shown in Fig. 2. Total three lenses including an objective lens with a large numerical aperture of 0.55 for large Δk collection are used for imaging far-field plane on the entrance slit of the spectrometer. By imaging the far-field plane, the radial coordinate corresponds to the PL emission angle from the sample; in-plane momentum $k_{||} = 2\pi/\lambda \sin\theta$ of the polariton or the photon in the sample, where λ is the PL wavelength and θ is the PL emission angle. By using a spectrometer, the horizontal direction is deflected by a grating as energy axis. Since vertical axis corresponds to in-plane momentum, dispersion relation is measured by a CCD camera attached at the exit of the spectrometer. When we use the other exit of the spectrometer, PL enters the Hanbury-Brown and Twiss (HBT) setup for the second-order correlation function measurements. The HBT setup consists of a beam splitter, single photon detectors (Perkin Elmer, SPCM-AQRH-14) and a time-interval analyzer (ORTEC, picosecond time analyzer 9308). The spectrometer grating is adjusted every measurement at each temperature and pump laser power to obtain PL. The width of the spectrometer exit slit is set to obtain sufficiently wide spectrum by HBT setup ($\sim$4 nm). The detection width of in-plane momentum is $\Delta k \sim 2 \times 10^4$/cm.

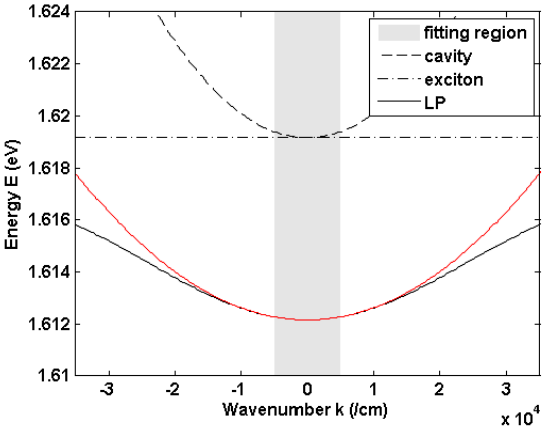

Figure 3. Evaluation on an accuracy of fitting between $E_{LP}(k_{\|}) = 1/2\big[E_{exc}(k_{\|}) + E_{cav}(k_{\|}) - \sqrt{4\hbar^2\Omega^2 + (E_{exc}(k_{\|}) - E_{cav}(k_{\|}))^2}\big]$ (solid black curve) and a fitting quadratic curve (red curve). Then, we evaluate a relative error and a theoretical effective mass. This fitting is using 29 data points from the region $|k_{\|}| < 0.5 \times 10^4$/cm. The effective mass by fitting is 7.48×10^{-35} kg and the relative error is 0.26 %. From this evaluation, we analyze experimental data points from the region $|k_{\|}| < 0.5 \times 10^4$/cm to evaluate the effective mass.

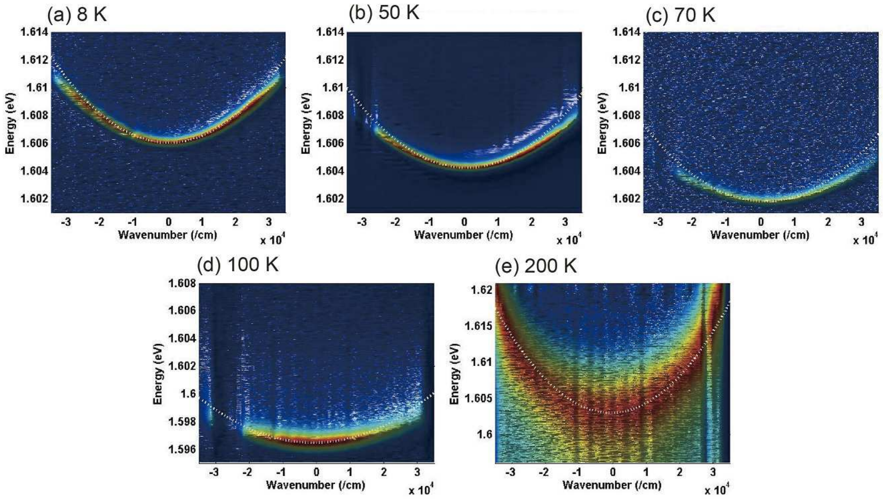

Figure 4. Dispersion relations below threshold at several temperatures. At (a) 8 K, (b) 50 K, (c) 70 K and (d) 100 K, the dispersion is LP branch. The cavity mode branch dispersion is observed at (e) 200 K. As temperature increases (a)-(d), the effective mass is heavier and the detuning is larger. This is because the energy of exciton red-shift by increasing temperature is faster than one of cavity. At 200K, the effective mass is the mass of cavity photon since strong coupling no longer exists due to large detuning and the system is in weak coupling regime.

Table 2. Effective mass and detuning dependences on temperature.

	8 K	50 K	70 K	100 K	200 K (cavity)
effective mass (10^{-35} kg)	6.9	7.7	8.2	12.4	2.8
detuning (meV)	2.5	3.8	4.5	9.0	-

4.2. Temperature dependence below threshold

In this section, temperature dependences of normal modes' dispersion relations at various temperatures are seen in the low excitation regime below the condensation or lasing threshold. As temperature increases, both exciton energy and cavity photon energy show red-shift. The exciton energy red-shift is faster than one of the cavity photon energy. The detuning $\Delta E(k_{\|}) = E_{cav}(k_{\|}) - E_{exc}(k_{\|})$, where $E_{\mathrm{cav}}(k_{\|})$ is the cavity photon energy and $E_{\mathrm{exc}}(k_{\|})$ is the exciton energy becomes larger as the system temperature increases. The effective mass of LP is described by $1/m_{LP} = |X|^2/m_{exc} + |C|^2/m_{cav}$ where $|X|^2$ and $|C|^2$ are the Hopfield coefficients determined by detuning and normal mode splitting $2\hbar\Omega$. Here, the effective mass of exciton m_{exc} is defined by $1/m_{exc} = 1/m_e + 1/m_{hh}$ with the electron mass m_e, the heavy hole (hh) mass m_{hh} and the effective mass of cavity photon m_{cav}. From dispersion relations, the effective mass m^* is calculated by $1/m^* = (1/\hbar^2)d^2E(k)/dk^2$. In the region $k_{\|} \ll k_{\perp}$, the energy of cavity mass $E_{cav} = \hbar c/n_c({k_{\|}}^2 + {k_{\perp}}^2)^{1/2}$ is approximated by the quadratic curve. Thus, the effective mass in $k_{\|} = 0$ is $m_{cav} = 2\pi\hbar {n_c}^2/(\lambda_c c)$ with a refractive index n_c and a resonant frequency λ_c. The effective mass at the bottom of the LP branch is 7.46 $\times 10^{-35}$ kg. The following parameters are used : $2\hbar\Omega = 14$ meV, $m_e = 0.0665 m_0$, $m_{hh} = 0.111 m_e$, free electron mass $m_0 = 9.109 \times 10^{-31}$ kg, $\lambda_c = 767.5$ nm, $n_c = 3.6$ for GaAs and $\Delta E = 0$.

We experimentally measure dispersion curves, and fit a quadratic curve to the dispersion curve near $k_{\|} = 0$ and estimate a effective mass from the curvature. In case of a LP branch, the wider a region of fitting points, the heavier a evaluated effective mass is. See Fig. 3 for the fitting region.

We perform a time-integrated far-field spectroscopy. Dispersions taken below threshold on various temperatures are shown in Fig. 4. These dispersions represent the transition from the light mass LP mode at 8 K to exciton-like heavier LP modes at high temperatures 50 K, 70 K and 100 K and then cavity mode at 200 K by increasing temperature. At 200 K, we show cavity photon mode because the lasing threshold is reached in this mode. Note that the lower branch turns from LP to exciton, then, no threshold behaviour is seen in the lower energy branch at 200 K. In what follows, we analyze the effective mass, the detuning and the refractive index. Table 2 shows the effective masses and the detunings. Here, the detuning is evaluated by the cavity photon mass at 200 K and the effective mass of LP at the temperature. The refractive index is 3.14 from the cavity photon mass at 200 K. The refractive index is lower than one of GaAs because the sample structure is layered DBR with GaAs, $Ga_{0.8}Al_{0.2}As$ and AlAs whose refractive indexes are smaller than one of GaAs. At 8 K, the detuning between the cavity mode and the exciton mode is 2.5 meV. In this situation, LPs relax to the bottom of the branch and form polariton condensate when the pump power is increased. As increasing temperature, 50 K, 70 K and 100 K, the effective mass becomes heavier and the detuning is larger. The LP mode becomes exciton-like because the exciton energy red-shift is faster than one of the cavity photon energy. After that, the LP mode seperate to the hh exciton mode and the cavity photon mode. At 200 K, the light effective mass shows the cavity photon mode. The separation means the transition from the strong coupling to the weak coupling.

4.3. Excitation density dependence

In this subsection, we will see dependences of normal modes on excitation density at several temperatures. As shown below, we will see distinct features of high density polariton condensates at the low temperature (8 K) from PL intensity, energy, linewidth and second-order correlation function to be compared with photon laser obtained at the high temperature (200 K). Also the various temperature data from 8 K to 200 K clearly show how each feature of polariton condensate becomes closer to and converges into the feature of photon laser.

4.3.1. PL intensity Excitation density dependences of PL intensity on pump laser power at various temperatures, 8 K, 50 K, 70 K, 100 K and 200 K, are shown in Fig. 5. Nonlinear PL intensity increase is seen at each temperature. As temperature increases, the threshold laser power, i.e., the threshold excitation density, also increases. Population inversion against the crystal ground state is necessary for photon lasing. Then the excitation density to reach lasing threshold becomes higher. On the other hand, in the polariton system, population inversion against the crystal ground state is not necessary [9]. Note that the normal modes below threshold for lower temperature than 100 K are LP and UP. And we see the lower branches reach the threshold. When we scan temperature from the lower to the higher, UP gradually changes to cavity mode and LP becomes exciton with very flat curvature of heavy effective mass. Then, the normal mode at 200 K is cavity due to dissociation of exciton and large detuning, that is, the cavity mode is already inside the conduction band. The cavity mode becomes the lasing mode at 200 K.

The 8 K case (Fig. 5a) has the lowest threshold pump power of around 3 mW. As excitation goes up further, monotonic increase of PL intensity is seen, however, a clear second threshold is not seen as shown in previous studies [10, 11, 12, 13, 14, 15, 16]. As temperature increases, the threshold also increases (Fig. 5b-d) as is known in thermal equilibrium theory of BEC. In the case of 50 K (Fig. 5b), the second threshold is not seen, either. However, it is seen at 70 K (Fig. 5c) where nonlinear PL intensity increase is seen above 300 mW implying the transition to photon laser. In 100 K and 200 K cases (Fig. 5d,e), the second threshold is not seen which implies the system has already

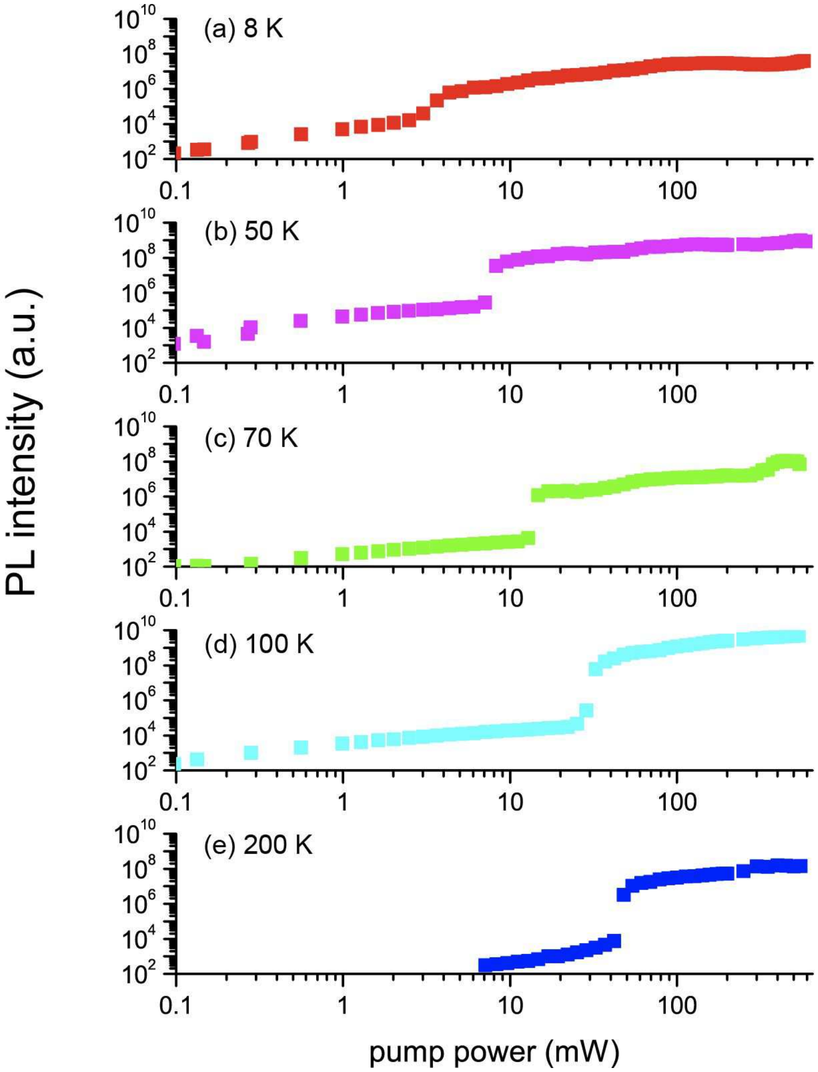

Figure 5. Excitation density dependence of PL intensity at k=0. (a) 8 K, (b) 50 K, (c) 70 K, (d) 100 K, (e) 200 K. In 200 K case, the PL intensity is weak and undetectable below 6mW

reached the photon lasing at the first threshold. However, it is unclear in the case of 100 K due to the property of the second-order correlation function as shown below.

4.3.2. PL energy Next, we see PL energy at $k = 0$ giving the maximum PL intensity at each temperature as shown in Fig. 6. The 8 K case (Fig. 6a) shows a blue-shift around the threshold ($\sim$ 3 mW) starting from the energy below the condensation threshold ($\sim$1.608 eV). The energy gradually approaches the cavity photon energy at 1.615 eV. Interesting behaviours are seen at 50 K (Fig. 6b). The condensation threshold is around 6 mW. Note that the energy below the threshold shows red-shift due to temperature increase. Then large blue-shift of 5 meV occurs. The degree of the blue-shift is much larger than 8 K case. The reason can be attributed to the large excitonic component at this temperature resulting in large interaction energy. As further increasing excitation

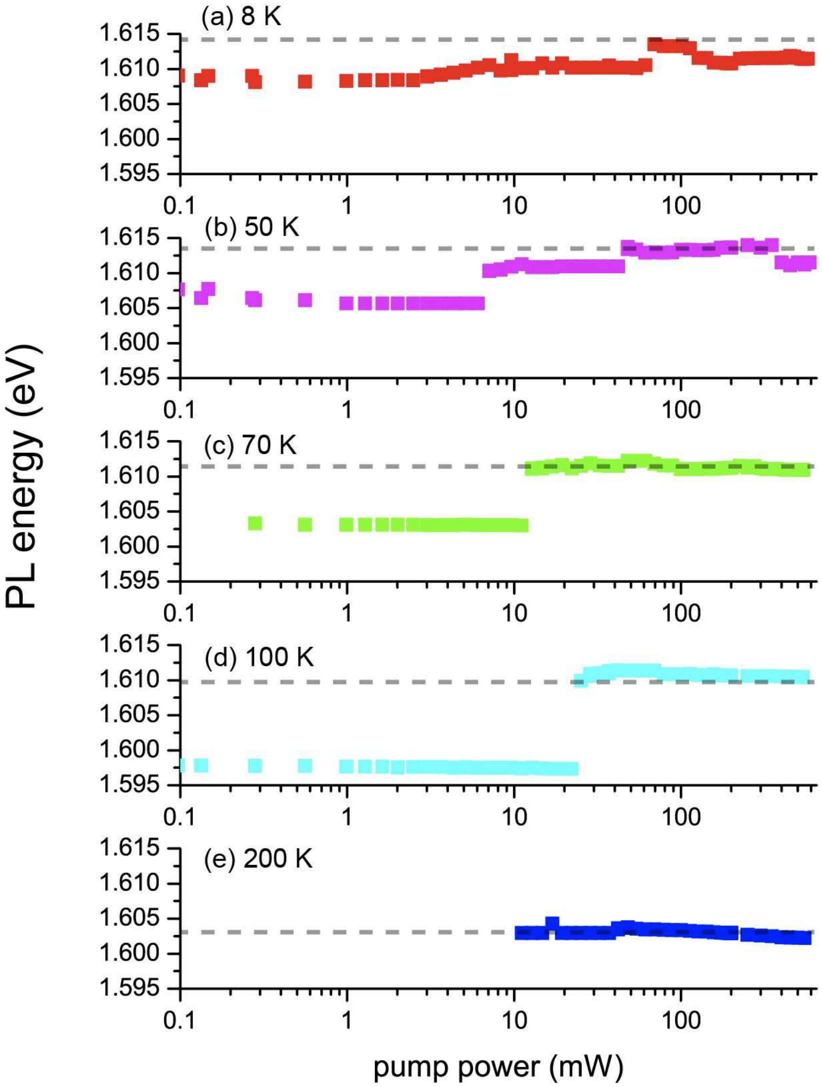

Figure 6. Excitation density dependence of PL energy. Dashed line is the energy of cavity photon of k=0 at each temperature. The discrepancy between the dashed line at 100 K and the PL energy above threshold is due to the precision of the cavity energy evaluation calculated from the effective mass. The limitation to the precision comes from the broad linewidth due to the thermal energy.

density, the PL energy around 40 mW pump power becomes larger than one below the condensation threshold pump power by 7 meV and reaches the cavity photon energy. However, even in this condition, the lower energy peak (5 meV higher than the energy below threshold) does not disappear and becomes stronger at the highest excitation regime around 400 mW as is also seen in 8 K. Due to the pulse laser pumping, polariton density experiences pulsed profile with time in the scale of 1-10 ps. Then, the PL at maximum excitation density is emitted from cavity photon energy, while PL shows lower energy as density decreases.

In the case of 70 K (Fig. 6c), situation becomes different. The large blue-shift is

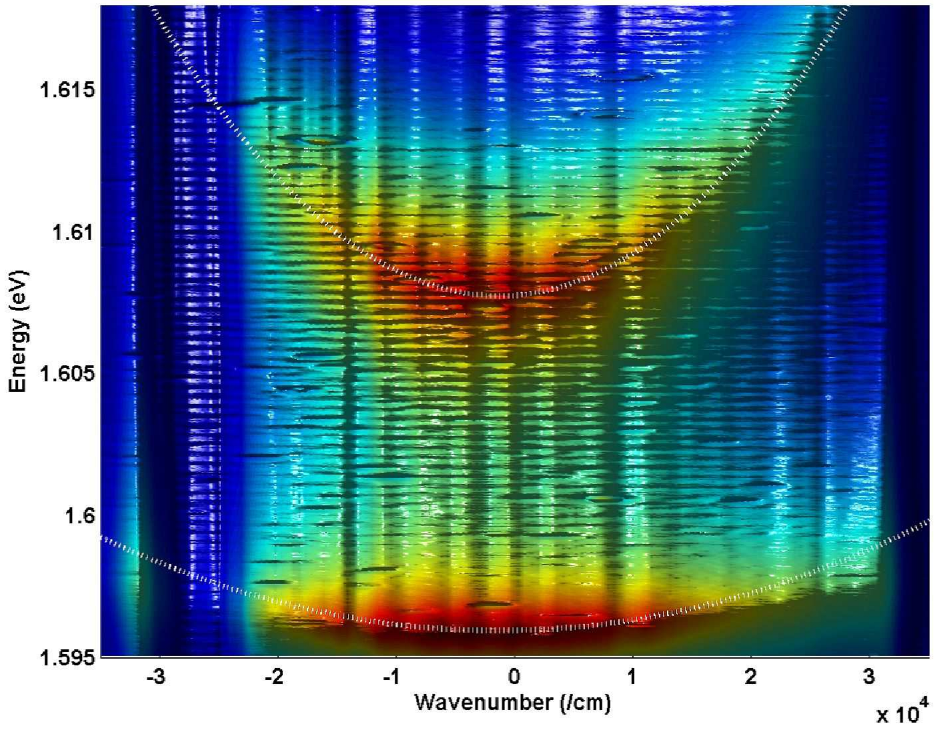

Figure 7. Dispersion around threshold at 100 K.

7 meV at the threshold around 10 mW. There is no longer large change in the energy in high excitation regime. This may be because the system is heated by a strong pump laser. The system remains in the weak coupling regime even the excitation density is decreased with the pulsed excitation profile. At the second threshold seen in PL intensity (Fig. 5c), the energy giving maximum PL intensity does not change and stays at cavity photon energy. However, the fact of PL intensity second threshold casts the possibility of the difference from photon laser at regime between the first threshold (∼10 mW) and the second threshold (∼300 mW).

The 100 K case (Fig. 6d) shows a similar behaviour with the 70 K case except the degree of the blue-shift at the threshold. In low temperature cases, the normal mode splitting is 14 meV and the cavity photon energy is around the center between UP and LP. However, the detuning is large at this temperature and the cavity photon energy is very close to the UP energy. Therefore, the blue-shift at the threshold from LP energy to cavity photon energy is larger than one of lower temperatures and almost the degree of normal mode splitting. In Fig. 7, the curvature of lower energy mode shows heavy LP mass due to the large detuning at 100 K while upper energy mode shows the curvature of the cavity photon mode which is brighter around the threshold pump power. The energy above threshold is one of the cavity photon energy implying a photon lasing.

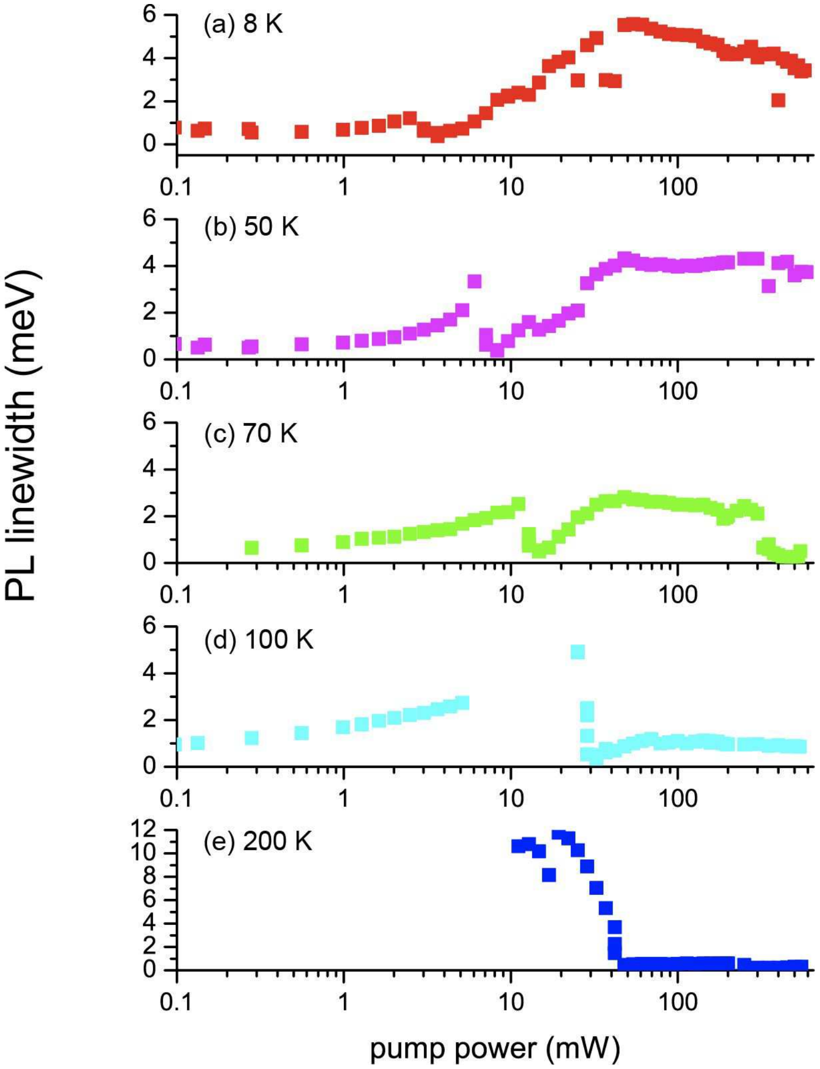

Figure 8. Excitation density dependence of PL linewidth.

4.3.3. PL linewidth In 8 K case (Fig. 8a), narrowing of energy linewidth at threshold is seen. Linewidth broadening is seen as the density increases due to the following reasons. One reason is the polariton-polariton interaction effect [30], and the other is the pulsed excitation since the degree of the blue-shift depends on the excitation density and the PL from various densities are integrated at the CCD attached to the spectrometer. Then, it results in the broader linewidth. The gradual narrowing of linewidth around the highest density regime shows the possibility of the concentration on the cavity photon energy and decrease of polariton-polariton interaction, which means the approach to photon lasing. Similar behaviour is seen in 50 K (Fig. 8b), i.e. narrowing of linewidth at the condensation threshold and following broadening due to the above mentioned reasons. When the maximum PL energy comes to the cavity photon energy around 40 mW (Fig. 6b), the broadening stops. But the linewidth is not so narrow but stays at large value around 4 meV as in the case of 8 K. This is caused by the fact that the PL comes from not only the cavity photon energy but also the lower energy as discussed in the previous subsection. While narrowing of linewidth at threshold and following broadening is also seen at 70 K (Fig. 8c), the maximum linewidth less than 3 meV is smaller than ones of lower temperatures. This is due to the fact that there is only one peak at the cavity photon energy. However, this is still quite larger than photon lasing case (see 200 K case) and implies the possibility of polariton-polariton interaction effect remaining. At the second threshold around 300 mW, narrowing due to the PL concentration on the cavity photon energy is seen. The clear transition to photon lasing occurs. At 100 K (Fig. 8d), narrowing occurs at threshold, however, following broadening is further smaller than 70 K caused by the decrease of polariton-polariton interaction effect. The case of 200 K (Fig. 8e) shows broad linewidth below threshold caused by large thermal energy and narrowing at lasing threshold. PL energy is always the cavity photon energy since there is no polariton-polariton interaction effect. Therefore, no broadening of linewidth occurs above lasing threshold.

In summary, while narrow linewidth is seen at higher temperature than 70 K, low temperature cases (8 K and 50 K) show broad linewidth even in the highest excitation regime, which implies the possibility that polariton-polariton interaction still remains even at the high density regime of the order of a hundred times the condensation threshold.

4.3.4. Second-order correlation function At the last part of this section, results of second-order correlation function experiments are shown in Fig. 9. The measurements were done in HBT setup, however, the difficulty of detecting weak signals prevented the determination of values at small pump powers. In the case of 8 K (Fig. 9a), PL shows bunching behaviour above threshold ($g^{(2)}(0) > 1$) [3, 22, 28, 16] until high excitation density regime. In this study, the bunching remains up to more than a hundred times of the condensation threshold (>300 mW). When the measurements are performed using a high time-resolution streak camera [16], the $g^{(2)}(0)$ below threshold becomes closer to two by correctly obtaining the statistics of thermal state. However, in the present study, the signal in one pulse is not time-resolved due to the time-resolution (∼300 ps) of the photon detectors of the HBT setup. The statistics is averaged out since the intensity correlation time is much shorter than the PL lifetime; the correlation between the photon at the beginning of the PL pulse and the end of the pulse is not seen. Our $g^{(2)}(0)$ results in the unity. On the other hand, when the system is in condensation regime, the PL pulse width is shortened more than one order of magnitude. The intensity correlation time of the system covers the entire pulse of PL. Therefore, despite the time-resolution of the detectors are still longer than the PL lifetime, the detection system correctly obtains the photon statistics [22, 28]. Bunching at broad excitation density regime is also seen at 50 K (Fig. 9b). However, the large bunching above threshold at 70 K (Fig. 9c) is quite different from low temperatures. The behaviours are similar with the case of a photon lasing. The $g^{(2)}(0)$ does not reach the unity. Instead, the second increase above the second threshold is seen as also shown in the previous study [16]. At 100

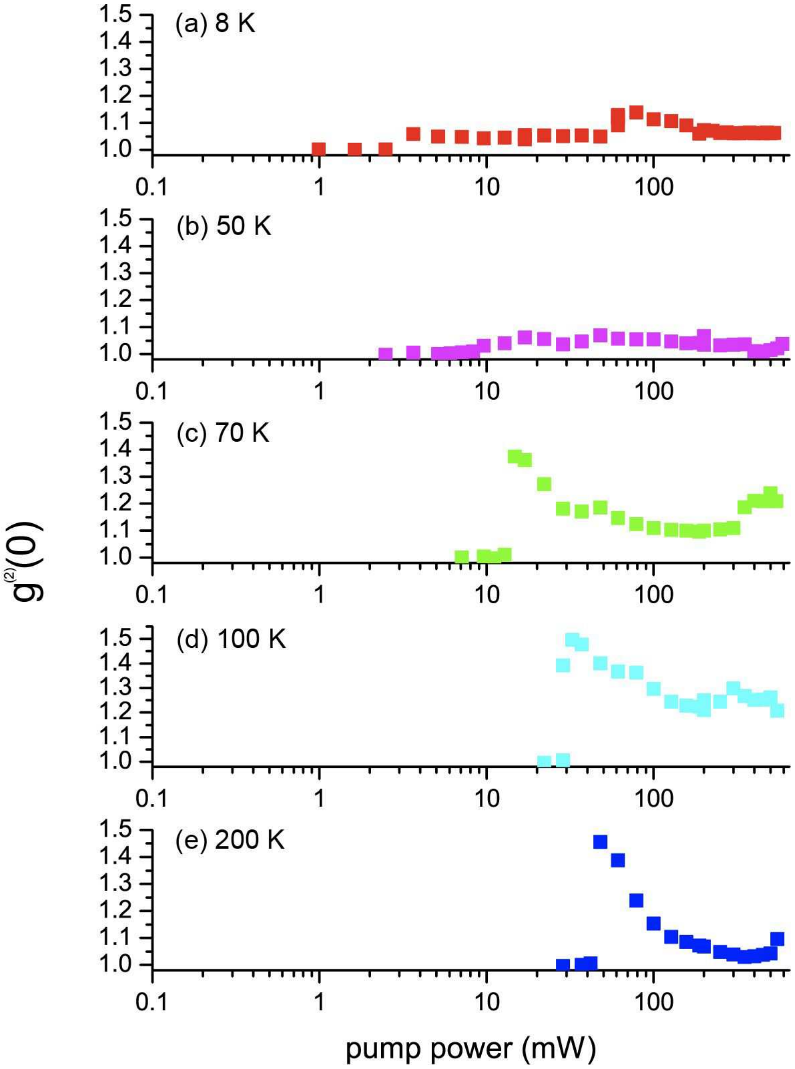

Figure 9. Excitation density dependence of second-order coherence function.

K (Fig. 9d), since there is no clear second threshold in PL intensity, no clear second threshold of $g^{(2)}(0)$ is, either. However, the clear convergence into the unity is not seen at this tempereture, implying the difference from photon lasing. Further higher density may cause the convergence, though. In the case of 200 K (Fig. 9e), $g^{(2)}(0)$ takes the transition at the threshold and monotonically decreases to the unity. These are typical characteristics of photon lasing [21].

5. Conclusion and Discussion

We have observed exciton-polariton system at various temperatures and excitation densities. The results are summarised in Table 3, which shows the possibility of polariton condensation up to the high excitation regime at low temperatures. The characteristics of low temperature data differ from photon lasing conventionally obtained at high temperatures. At intermediate temperatures, some characteristics are in common with low temperatures and some are not, showing the possibility of intermediate phase between polariton condensation and photon lasing. This study opens up a new study of polariton condensate in high excitation regime.

Table 3. Different phase transitions at various temperatures.

	first threshold	second threshold
8 K	polariton condensation	
50 K	polariton condensation	
70 K	polariton condensation	photon lasing
100 K	photon lasing?	
200 K	photon lasing	

The possibility of the new phase in the high excitation regime has been theoretically studied in the nonequilibrium condition [20] by using the framework developed in Ref. [29]. Though we have not obtained the direct evidence of e-h pair correlation in the high excitation regime, recent observations of ghost polariton branch [31, 32] by using a intense resonant excitation laser give the possibility of e-h pair binding and polariton even in the high density regime.

Acknowledgments

The authors wish to acknowledge T. Ogawa, T. Byrnes, K. Kamide, M. Yamaguchi, N. Ishida for their helpful comments. This research is supported by the Japan Society for the Promotion of Science (JSPS) through its FIRST Program and KAKENHI Grant Number 24740277, a Space and Naval Warfare Systems (SPAWAR) Grant N66001-09-1-2024, the Ministry of Education, Culture, Sports, Science, and Technology (MEXT),State of Bavaria, the National Institution of Information and Communication Technology (NICT), and the joint research program at Institute for Molecular Science.

References

[1] Snoke D and Littlewood P B 2010 *Physics Today* **63** 42
[2] Deng H, Haug H and Yamamoto Y 2010 *Rev. Mod. Phys.* **82** 1489
[3] Deng H, Weihs G, Santori C, Bloch J and Yamamoto Y 2002 *Science* **298** 199
[4] Kasprzak J, et al. 2006 *Nature* **443** 409
[5] Amo A, *et al.* 2009 *Nature* **457** 291
[6] Lagoudakis K G, Wouters M, Richard M, Baas A, Carusotto I, André R, Dang L S and Deveaud-Plédran B 2008 *Nat. Phys.* **4** 706
[7] Roumpos G, Fraser M D, Löffler A, Höfling S, Forchel A and Yamamoto Y 2011 *Nat. Phys.* **7** 129
[8] Utsunomiya *et al.* 2008 *Nat. Phys.* **4** 700
[9] Imamoglu A, Ram R J, Pau S and Yamamoto Y 1996 *Phys. Rev. A* **53** 4250
[10] Dang L S, Heger D, André R, Bœuf F and Romenstein R 1998 *Phys. Rev. Lett.* **81** 3920

[11] Deng H, Weihs G, Snoke D, Bloch J and Yamamoto Y 2003 *Proc. Natl. Acad. Sci. USA* **100** 15318

[12] Bajoni D, Senellart P, Lemaître A and Bloch J 2007 *Phys. Rev. B* **76** 201305(R)

[13] Nelsen B, Balili R, Snoke D, Pfeiffer L and West K 2009 *J. Appl. Phys.* **105** 122414

[14] Bajoni D, Senellart P, Wertz E, Sagnes I, Miard A, Lemaître A and Bloch J 2008 *Phys. Rev. Lett.* **100** 047401

[15] Kammann E, Ohadi H, Maragkou M, Kavokin A V and Lagoudakis P G 2012 *New J. Phys.* **14** 105003

[16] Tempel J S, Veit F, Assmann M, Kreilkamp L E, Rahimi-Iman A, Löffler A, Höfling S, Reitzenstein S, Worschech L, Forchel A and Bayer M 2012 *Phys. Rev. B* **85** 075318

[17] Kamide K and Ogawa T 2010 *Phys. Rev. Lett.* **105** 056401

[18] Byrnes T, Horikiri T, Ishida N, Yamamoto Y, 2010 *Phys. Rev. Lett.* **105** 186402

[19] Kamide K and Ogawa T 2011 *Phys. Rev. B* **83** 165319

[20] Yamaguchi M, Kamide K, Ogawa T and Yamamoto Y 2012 *New J. Phys.* **14** 065001

[21] Ulrich S M, Gies C, Ates S, Wiersig J, Reitzenstein S, Hofmann C, Löffler A, Forchel A, Jahnke F and Michler P 2007 *Phys. Rev. Lett.* **98** 043906

[22] Kasprzak J, Richard M, Baas A, Deveaud B, André R, Poizat J -Ph and Dang L S 2008 *Phys. Rev. Lett.* **100** 067402

[23] Schwendimann P and Quattropani A, 2008 *Phys. Rev. B* **77** 085317

[24] Sarchi D, Schwendimann P and Quattropani A 2008 *Phys. Rev. B* **78** 073404

[25] Doan T D, Thien Cao H, Tran Thoi D B and Haug H 2008 *Phys. Rev. B* **78** 205306

[26] Wouters M and Savona V, 2009 *Phys. Rev. B* **79** 165302

[27] Haug H, Doan T D, Thien Cao H, and Tran Thoai D B 2012 *Phys. Rev. B* **85** 205310

[28] Horikiri T, Schwendimann P, Quattropani A, Löffler A, Höfling S, Forchel A and Yamamoto Y 2010 *Phys. Rev. B* **81** 033307

[29] Szymańska M H, Keeling J, and Littlewood P B 2006 *Phys. Rev. Lett.* **96**, 230602

[30] Porras D and Tejedor C, 2003 *Phys. Rev. B* **67** 161310(R)

[31] Kohnle V, Léger Y, Wouters M, Richard M, Portella-Oberli M T and Deveaud-Plédran 2011 *Phys. Rev. Lett.* **106** 255302

[32] Zajac J M and Langbein W, 2012 arXiv:1210.1455